Scientific Research Publishing

Open Journal of Applied Sciences, 2024, 14, 818-832
https://www.scirp.org/journal/ojapps
ISSN Online: 2165-3925
ISSN Print: 2165-3917

Research on the Damping Mechanism of Time-Delay Coupled Negative Stiffness Dynamic Absorber in Nonlinear Vibration Damping System

Weikai Wang, Yanying Zhao, Qiqi Li, Hao Wu, Liuqing Yang

School of Aircraft Engineering, Nanchang Hangkong University, Nanchang, China
Email: www.wwk2506099838@163.com

How to cite this paper: Wang, W.K., Zhao, Y.Y., Li, Q.Q., Wu, H. and Yang, L.Q. (2024) Research on the Damping Mechanism of Time-Delay Coupled Negative Stiffness Dynamic Absorber in Nonlinear Vibration Damping System. *Open Journal of Applied Sciences*, **14**, 818-832.
https://doi.org/10.4236/ojapps.2024.144055

Received: March 10, 2024
Accepted: April 6, 2024
Published: April 9, 2024

Abstract

A study was conducted on the effect of time delay and structural parameters on the vibration reduction of a time delayed coupled negative stiffness dynamic absorber in nonlinear vibration reduction systems. Taking dynamic absorbers with different structural and control parameters as examples, the effects of third-order nonlinear coefficients, time-delay control parameters, and negative stiffness coefficients on reducing the replication of the main system were discussed. The nonlinear dynamic absorber has a very good vibration reduction effect at the resonance point of the main system and a nearby area, and when 1 increases to a certain level, the stable region of the system continues to increase. The amplitude curve of the main system of a nonlinear dynamic absorber will generate Hop bifurcation and saddle node bifurcation in the region far from the resonance point, resulting in almost periodic motion and jumping phenomena in the system. For nonlinear dynamic absorbers with determined structural parameters, time-delay feedback control can be adopted to control the amplitude of the main system. For different negative stiffness coefficients, there exists a minimum damping point for the amplitude of the main system under the determined system structural parameters and time-delay feedback control parameters.

Keywords

Time Delay, Nonlinear, Dynamic Vibration Absorber

1. Introduction

The time-delay dynamic vibration absorber is a new technology, which intro-

duces a partial state feedback with time delay to the vibration absorber based on the traditional dynamic vibration absorber, which belongs to the semi-active vibration control in essence. The advantage of time-delay dynamic vibration absorber is that the frequency range of vibration reduction is large, it can be adjusted in real-time, and in some cases (such as when applied to the structure vibration reduction of the main system is a single degree of freedom) it can completely absorb the vibration of the main system, and the time-delay dynamic vibration absorber is easy to design. However, at present, the theoretical and experimental research on vibration reduction of amplifying mechanism absorbers with additional negative stiffness is not in-depth. Therefore, mechanism analysis and optimization design are carried out to provide a theoretical basis for the design of new dynamic vibration absorber models. Domestic and foreign scholars have done relevant research on the design optimization and time-delay application of vibration absorbers.

The traditional linear adjustable dynamic vibration absorber is a kind of vibration absorber which is placed on the main system and absorbs the energy of the main system. The vibration control can be divided into passive control, active control and semi-active control according to its components. The passive control device is widely used for its advantages of simple structure, strong stability and no external energy supply. The stiffness and damping of the early passive vibration control devices are linear, so when the environmental excitation is random or broadband, the vibration reduction effect will be sharply reduced due to frequency imbalance. The first undamped vibration absorber was proposed by Frahm [1] to completely suppress the amplitude of the main system by generating anti-resonance at the target frequency, but the effective frequency regulation range is only in a narrow frequency band near the anti-resonance point. Den Hartog *et al.* [2]: Adding damping to the absorber not only overcomes the disadvantage of narrow band of the undamped absorber, but also effectively inhibits the amplitude of the main system. The finding that the frequency response curve of the main system always passes through two fixed points and is not affected by the damping value of the absorber provides the support of the fixed-point theory for the optimization of structural parameters. Asami *et al.* [3] [4] adopted the fixed-point theory to optimize the structural parameters of the damped vibration absorber on the premise that the amplitudes of the two formant peaks were equal and minimum, and obtained the exact solution of the optimal structural parameters of the vibration absorber. Literature [5] designed a vibration isolation system with negative stiffness structure by using the principle of parallel cancellation of positive stiffness, and derived the stiffness criterion of static stability of the elastic system by using the energy criterion, proving that the negative stiffness system has the advantages of low natural frequency, large bearing capacity and good vibration isolation effect. Peng Haibo *et al.* [6] optimized the parameters of the dynamic vibration absorber system containing negative stiffness elements, and obtained the optimal frequency ratio and optimal damping ratio of the negative stiffness vibration absorber by using the fixed-point

theory. The research shows that the negative stiffness dynamic vibration absorber has stronger damping capacity and wider damping frequency band than the traditional dynamic vibration absorber. Wang Xiaoran *et al.* [7] optimized the parameters of a three-element dynamic vibration absorber containing a negative stiffness spring element, adjusted the three fixed points to the same amplitude by using the fixed-point theory, and obtained the optimal negative stiffness ratio. The shock absorber has good vibration damping performance. Hao Yan *et al.* [8] optimized the parameters of the Maxwell model dynamic vibration absorber for devices with negative stiffness, and adjusted the three fixed points to the same amplitude by using the fixed-point theory to obtain the optimal negative stiffness ratio. The shock absorber can greatly reduce the amplitude of the resonance region and has a wide damping frequency band. Xing Zhaoyang *et al.* [9] combined the lever amplification mechanism with the negative stiffness structure, which can greatly reduce the resonance amplitude, broaden the damping frequency band, and reduce the resonant frequency of the system. Chen Jie *et al.* [10] used a dynamic vibration absorber containing a inertial vessel and negative stiffness to suppress the transverse vibration of the beam. The negative stiffness can suppress the vibration of the beam well, while the inertial vessel can further inhibit the vibration. Some scholars have found that taking time delay as a state feedback control quantity, consciously controlling its size, and making it reasonably matched with the feedback system can have a good vibration reduction effect. Many scholars have done a lot of research on time delay in vibration control systems. Li Yingsong *et al.* [11] designed a new type of magnetic liquid damper and studied the influence of different factors on the performance of the magnetic liquid damper. Based on the existing dynamic vibration absorber, Li Yan [12] added a particle damping system, hollowing out the original mass blocks and filling in particle materials to form a particle damping dynamic vibration absorber, and studied its effect on vibration and noise reduction in the track structure. Yang Geng *et al.* [13] proposed a dynamic vibration absorber with multiple dry friction damping with compact structure and designed a ring vibration absorber structure composed of multiple cantilever beam type vibrators to solve the vibration suppression problem when the rotor was over critical speed. Then, the nonlinear dynamic equation of the absorber is constructed by Lagrange equation and integrated with the finite element model of the rotor structure, and the coupling dynamic equation of the absorber and rotor system is obtained. On this basis, the influence of vibration absorber parameters on its vibration damping performance is analyzed to clarify the vibration damping characteristics of multiple dry friction damping vibration absorber. Xiong Bo *et al.* [14] built a double-wire pendulum test system to explore the vibration damping performance of the hub double-wire pendulum absorber on the test bench, and conducted a comparison of vibration levels under the no-axis rotation test of the test bench and the double-wire pendulum test respectively. The results showed that the maximum vibration absorption effect of the double-wire pendulum on the bearing seat of the test bench could reach 35% under single-direction loading.

When Fx and Fy are loaded in the same direction, the maximum vibration absorption effect can reach 61%. Olgac *et al.* [15] applied the time-delay feedback as an input to the vibration absorber to form a "time-delay dynamic vibration absorber". Simulation shows that the vibration reduction effect of the vibration absorber with time-delay feedback is better than that of the passive vibration absorber. Teacher Zhao Yanying [16] studied the damping effect of time-delay dynamic vibration absorber on the main system in nonlinear vibration system by taking advantage of the active control with time delay. Sun *et al.* [17] verified the effectiveness of delay damping through experiments. Chen Longxiang *et al.* [18] studied the time-delay active control of the rotational motion and forced vibration of flexible beams. Subsequently, Chen Long *et al.* [19] studied the effect of time delay on semi-active suspension. Fu Wenqiang *et al.* [20] explored the asymptotic stability mechanism of the semi-active suspension control system with time-delay ceiling damping. Zhu Kun *et al.* [21] improved vehicle suspension performance based on tire displacement delay feedback control. Yan Gai *et al.* [22] considered the inherent time delay of the suspension system and applied the time-delay feedback to vehicle suspension control by using the state change method. Zhao Yanying *et al.* [23] studied the nonlinear time-delay feedback control of high-speed train with the vehicle body as the feedback object. Wu Kaiwei *et al.* [24] to address the issue of damage to vehicle components and impact on passenger comfort caused by vibrations generated during uneven road driving, a damping method for an active suspension with time-delay feedback control is proposed in a quarter car model.

2. Structural Model

Dynamic shock absorber is a kind of widely used shock absorber. Although the dynamic absorber can eliminate the vibration of the main system at the resonance point in a linear system, the damping effect is poor at the departure from the resonance point. To solve the problem that the linear dynamic absorber is not effective in damping the vibration far from the resonance point, the nonlinear dynamic absorber is used. Therefore, in this paper, the vibration suppression of the main system is studied under the coupling delay of the negative stiffness absorber with two degrees of freedom. The kinetic model is shown in the figure.

As shown in **Figure 1**, The whole system consists of main system m_1 and shock absorber m_2. C_1 is the damping coefficient of the main system, C_2 is the damping coefficient of the shock absorber. The spring of the main system is linear and its stiffness coefficient is K_1. The spring of the shock absorber is nonlinear, and the expression of the nonlinear elastic element is $f = k_2\delta + \beta_1\delta^3$, where K_2 is the linear stiffness coefficient of the shock absorber, and β_1 is the nonlinear stiffness coefficient of the shock absorber. K_3 is the introduced negative grounding stiffness. Assuming that the main system receives an external excitation the period $f(t) = A\cos\omega t$, $x_1(t)$ and $x_2(t)$ represent the vertical displacement of the main system and the absorber. Is the delay feedback control,

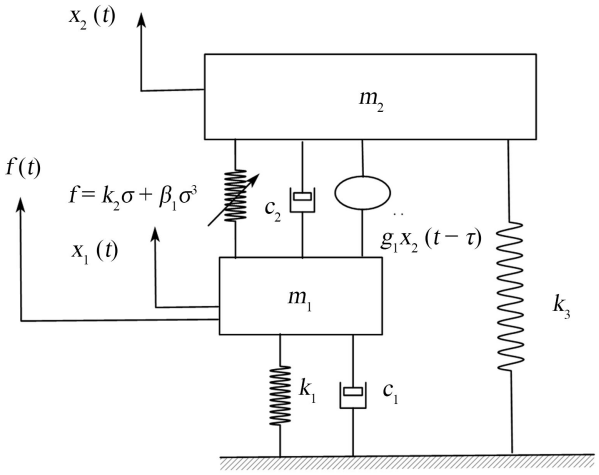

Figure 1. Nonlinear model of time-delay coupled negative stiffness dynamic vibration absorber.

where g is the delay feedback gain coefficient and τ is the delay quantity.

The dynamic equation of the vibration absorber system is as follows:

$$\begin{aligned} &m_1\ddot{x}_1 + k_1x_1 + c_1\dot{x}_1 + k_2(x_1 - x_2) + \beta_1(x_1 - x_2)^3 + c_2(\dot{x}_1 - \dot{x}_2) - g_1\ddot{x}_{2\tau} = f(t) \\ &m_2\ddot{x}_2 + k_2(x_2 - x_1) + \beta_1(x_2 - x_1)^3 + c_2(\dot{x}_2 - \dot{x}_1) + k_3x_2 + g_1\ddot{x}_{2\tau} = 0 \end{aligned} \tag{1}$$

where, $x_{2\tau} = x_2(t-\tau)$, when the gain coefficient of hysteretic feedback is $g_1 = 0$, the delay feedback term of the system disappears.

3. Perturbation Analysis

To simplify the calculation, the following dimensionless quantities are introduced:

$$v_1 = \frac{c_1\Omega}{m_1\omega}, v_2 = \frac{c_2\Omega}{m_2\omega}, \alpha^* = \frac{\beta_1x_c^2\Omega^2}{m_2\omega^2}, \gamma = \frac{m_2}{m_1}, f = \frac{A\Omega^2}{m_1x_c\omega^2}, g^* = \frac{g_1\Omega^2}{m_2\omega^2},$$

$$\tau^* = \frac{\omega}{\Omega}\tau, t^* = \frac{\omega}{\Omega}t, y_1 = \frac{x_1}{x_c}, y_2 = \frac{x_2}{x_c}, \omega_1^2 = \frac{k_1\Omega^2}{m_1\omega^2}, \eta = \frac{k_3}{k_2}$$

where Ω is the dimensionless frequency, t^* is denoted as t and τ^* is denoted as τ for ease of writing. To facilitate perturbation analysis, some system variables are re-scaled:

$$v = \varepsilon\xi, \alpha^* = \varepsilon\alpha, \gamma = \varepsilon\mu, f = \varepsilon F, g^* = \varepsilon g, \eta = \varepsilon\zeta$$

where $0 < \varepsilon \le 1$ The dimensionless motion equation of the equation is:

$$\begin{aligned} \ddot{y}_1 + \omega_1^2y_1 = &-\varepsilon\xi_1\dot{y}_1 + \varepsilon\mu\omega_2^2(y_2 - y_1) + \varepsilon^2\mu\xi_2(\dot{y}_2 - \dot{y}_1) \\ &+ \varepsilon^2\mu\alpha(y_2 - y_1)^3 + \varepsilon^2\mu g\ddot{y}_{2\tau} + \varepsilon F\cos(\Omega t) \end{aligned} \tag{2}$$

$$\ddot{y}_2 + \omega_2^2(y_2 - y_1) = -\varepsilon\xi_2(\dot{y}_2 - \dot{y}_1) - \varepsilon\alpha(y_2 - y_1)^3 - \varepsilon g\ddot{y}_{2\tau} - \varepsilon\zeta\omega_2^2y_2 \tag{3}$$

The multi-scale method is adopted to solve the equation. Introduce different time scales:

$$T_n = \varepsilon^n t \tag{4}$$

The inverse of t concerning time becomes the partial derivative of T_n, so:

$$\begin{aligned}\frac{\mathrm{d}}{\mathrm{d}t} &= D_0 + \varepsilon D_1 + \cdots \\ \frac{\mathrm{d}^2}{\mathrm{d}t^2} &= D_0{}^2 + 2\varepsilon D_0 D_1 + \cdots\end{aligned} \tag{5}$$

where $D_i = \partial/\partial T_i, i = 0,1$

Set the solution as follows:

$$\begin{aligned}y_1(t,\varepsilon) &= y_{11}(T_0,T_1) + \varepsilon y_{12}(T_0,T_1) + \cdots \\ y_2(t,\varepsilon) &= y_{21}(T_0,T_1) + \varepsilon y_{22}(T_0,T_1) + \cdots \\ y_{2\tau}(t,\varepsilon) &= y_{21\tau}(T_0,T_1) + \varepsilon y_{22\tau}(T_0,T_1) + \cdots\end{aligned} \tag{6}$$

Then, by substituting Equations (5) and (6) into Equations (2) and (3), and making the coefficients of the same power of ε equal, we get ε^0:

$$\begin{aligned}D_0^2 y_{11} + \omega_1^2 y_{11} &= 0 \\ D_0^2 y_{21} + \omega_2^2 (y_{21} - y_{11}) &= 0\end{aligned} \tag{7}$$

ε^0:

$$\begin{aligned}D_0^2 y_{12} + \omega_1^2 y_{12} &= -2D_0 D_1 y_{11} - \xi_1 D_0 y_{11} + \mu\omega_2^2 (y_{21} - y_{11}) + F\cos(\Omega T_0) \\ D_0^2 y_{22} + \omega_2^2 (y_{22} - y_{12}) &= -gD_0^2 y_{21\tau} - 2D_0 D_1 y_{21} - \xi_2 (D_0 y_{21} - D_0 y_{11}) \\ &\quad - \alpha\left(y_{21}^3 - y_{11}^3 + 3y_{21}y_{11}^2 - 3y_{21}^2 y_{11}\right) - \zeta\omega_2^2 y_{21}\end{aligned} \tag{8}$$

The general solution of Equation (8) can be expressed as:

$$\begin{aligned}y_{11} &= A(T_1)\mathrm{e}^{i\omega_1 T_0} + cc \\ y_{21} &= B(T_1)\mathrm{e}^{i\omega_2 T_0} + C(T_1)\mathrm{e}^{i\omega_1 T_0} + cc\end{aligned} \tag{9}$$

where $C = \left(\frac{\omega_2^2}{\omega_2^2 - \omega_1^2}\right)A$. Where $i = \sqrt{-1}$ and cc represent the conjugate complex numbers of the preceding terms. The external excitation and delay terms can be expressed in the complex form as follows:

$$\begin{aligned}F\cos\Omega T_0 &= \frac{1}{2}F\mathrm{e}^{i\Omega T_0} + cc \\ y_{21\tau} &= B_\tau(T)\mathrm{e}^{i\omega_1(T_0-\tau)} + C_\tau(T)\mathrm{e}^{i\omega_2(T_0-\tau)} + cc\end{aligned} \tag{10}$$

Assuming that τ and ε are both small, B_τ and C_τ are expanded according to Taylor to get:

$$\begin{aligned}B_\tau &= B(T_1 - \varepsilon\tau) = B(T_1) - \varepsilon\tau B'(T_1) + \frac{\varepsilon^2\tau^2}{2}B'' + \cdots \\ C_\tau &= C(T_1 - \varepsilon\tau) = C(T_1) - \varepsilon\tau C'(T_1) + \frac{\varepsilon^2\tau^2}{2}C'' + \cdots\end{aligned} \tag{11}$$

Substituting Equations (9)-(11) into Equation (8) is obtained:

$$\begin{aligned}D_0^2 y_{22} + \omega_2^2 y_{22} &= \omega_2^2 y_{12} + K_1\mathrm{e}^{i\omega_2 T_0} + K_2\mathrm{e}^{i\omega_1 T_0} + K_3\mathrm{e}^{i3\omega_1 T_0} + K_4\mathrm{e}^{i3\omega_2 T_0} \\ &\quad + K_5\mathrm{e}^{i(\omega_1+2\omega_2)T_0} + K_6\mathrm{e}^{i(\omega_2+2\omega_1)T_0} + K_7\mathrm{e}^{i(-\omega_2+2\omega_1)T_0} \\ &\quad + K_8\mathrm{e}^{i(-\omega_1+2\omega_2)T_0} + K_9\mathrm{e}^{i\omega_1(T_0-\tau)} + K_{10}\mathrm{e}^{i\omega_2(T_0-\tau)} + cc \\ D_0^2 y_{12} + \omega_1^2 y_{12} &= K_{11}\mathrm{e}^{i\omega_2 T_0} + K_{12}\mathrm{e}^{i\omega_1 T_0} + K_{13}\mathrm{e}^{i\Omega T_0} + cc\end{aligned} \tag{12}$$

where:

$$K_1 = -i\omega_2\left(\xi_2 B + 2B'\right) - \alpha\left(6AB\overline{A} - 6BC\overline{A} + 3B^2\overline{B} - 6AB\overline{C} + 6BC\overline{C}\right) - \zeta B\omega_1^2,$$

$$K_2 = -i\omega_1\left[\xi_2\left(C - A\right) + 2C'\right] + \alpha\left(3A^2\overline{A} - 6AC\overline{A} + 3C^2\overline{A} + 6AB\overline{B} - 6BC\overline{B}\right.$$

$$\left. - 3A^2\overline{C} + 6AC\overline{C} - 3C^2\overline{C}\right) - \zeta C\omega_1^2,$$

$$K_3 = \alpha\left(A^3 - 3A^2C + 3AC^2 - C^3\right), K_4 = -\alpha B^3, K_5 = \alpha\left(3AB^2 - 3B^2C\right),$$

$$K_6 = -\alpha\left(3A^2B - 6ABC + 3BC^2\right), K_7 = -\alpha\left(3A^2\overline{B} - 6AC\overline{B} + 3C^2\overline{B}\right),$$

$$K_8 = \alpha\left(3B^2\overline{A} - 3B^2\overline{C}\right), K_9 = gC\omega_1^2, K_{10} = gB\omega_2^2,$$

$$K_{11} = \mu\omega_2^2 B, K_{12} = \mu\omega_2^2\left(C - A\right) - 2A'i\omega_1, K_{13} = F/2,$$

And $\left(\right)' = \partial\left(\right)/\partial T_1 = \partial\left(\right)/\partial\left(\varepsilon t\right)$.

Both linear dynamic vibration absorber and nonlinear dynamic vibration absorber use main resonance and 1:1 internal resonance to reduce the vibration of the main system. Under normal circumstances, due to the influence of manufacturing and control technology, the control of internal resonance ratio inevitably has a certain deviation, so the harmonic solution parameter is introduced to represent the deviation value. At the same time, the harmonic parameters are introduced to represent the size of the damping frequency band.

$$\omega_2 = \omega_1 + \varepsilon\delta_1, \tag{13}$$

$$\Omega = \omega_2 + \varepsilon\delta_2 \tag{14}$$

Considering Equations (13) and (14), the conditions for solvability of Equations (12) are obtained:

$$\begin{aligned} &-i\omega_2\left(\xi_2 B + 2B'\right) - \alpha\left(6AB\overline{A} - 6BC\overline{A} + 3B^2\overline{B} - 6AB\overline{C} + 6BC\overline{C}\right) \\ &-\zeta B\omega_1^2 + \frac{\mu\omega_2^4}{\omega_1^2 - \omega_2^2}B + \left[-i\omega_1\xi_2\left(C - A\right) - 2i\omega_1 C'\right. \\ &+\alpha\left(3A^2\overline{A} - 6AC\overline{A} + 3C^2\overline{A} + 6AB\overline{B} - 6BC\overline{B} - 3A^2\overline{C} + 6AC\overline{C} - 3C^2\overline{C}\right) \\ &\left.-\zeta C\omega_1^2\right]\mathrm{e}^{-i\delta_1 T_1} - \alpha\left(3A^2\overline{B} - 6AC\overline{B} + 3C^2\overline{B}\right)\mathrm{e}^{-i2\delta_1 T_1} \\ &+\alpha\left(3B^2\overline{A} - 3B^2\overline{C}\right)\mathrm{e}^{i\delta_1 T_1} + gB\omega_2^2\mathrm{e}^{-i\omega_2\tau} + gC\omega_1^2\mathrm{e}^{-i\left(\omega_1\tau + \delta_1 T_1\right)} = 0 \end{aligned} \tag{15}$$

$$\mu\omega_2^2\left(C - A\right) - 2A'i\omega_1 + \mu\omega_2^2 B\mathrm{e}^{i\delta_1 T_1} + \frac{1}{2}F\mathrm{e}^{i\delta_2 T_1} = 0 \tag{16}$$

Equations (15) and (16) can be written in polar coordinates as follows:

$$A\left(T_1\right) = \frac{1}{2}a\left(T_1\right)\mathrm{e}^{i\theta\left(T_1\right)} \tag{17}$$

$$B\left(T_1\right) = \frac{1}{2}b\left(T_1\right)\mathrm{e}^{i\theta\left(T_1\right)} \tag{18}$$

Equations (17) and (18) are substituted into Equations (15) and (16), and the resulting result is obtained by separating the real part and the imaginary part:

$$a' = -\frac{1}{2}\xi_1 a - \frac{1}{2\omega_1}\mu\omega_2^2 b\sin\phi_2 + \frac{1}{2\omega_1}F\sin\phi_1, \tag{19}$$

$$b' = \frac{\omega_2}{2} gb\sin(\omega_2\tau) + \frac{1}{2\omega_2}\xi\omega_1(1-\gamma)a\cos\phi_2 + \frac{\omega_1^2}{2\omega_2} g\gamma\left[\sin(\omega_1\tau)\ a\cos\phi_2 - \cos(\omega_1\tau)a\sin\phi_2\right] + \frac{1}{\omega_2}\alpha\left[(L_1 - L_3)\sin\phi_2 - L_2\sin(2\phi_2)\right] - \frac{1}{2\omega_2}\zeta\gamma a\omega_1^2\sin\phi_2, \tag{20}$$

$$a\phi_1' = \delta_2 a + \frac{1}{2\omega_1}\mu\omega_2^2(\gamma-1)a + \frac{1}{2\omega_1}\mu\omega_1^2 b\cos\phi_2 + \frac{F}{2\omega_2}\cos\phi_2, \tag{21}$$

$$b(\phi_1' + \phi_2') = b(\delta_2 - \delta_1) + \frac{1}{2(\omega_1^2 - \omega_2^2)}\mu\omega_2^3 b - \frac{\omega_2}{2} gb\cos(\omega_2\tau) - \frac{1}{2\omega_2}\xi\omega_1(1-\gamma)a\sin\phi_2 - \frac{\omega_1^2}{2\omega_2} g\gamma\left[\sin(\omega_1\tau)a\sin\phi_2 + \cos(\omega_1\tau)a\cos\phi_2\right] - \frac{1}{\omega_2}\alpha\left[(L_1 + L_3)\cos\phi_2 + L_2\cos(2\phi_2) + L_4\right] - \frac{1}{2\omega_2}\zeta\left(b\omega_1^2 + \gamma a\omega_1^2\cos\phi_2\right) \tag{22}$$

4. Equilibrium Solution and Its Stability

The steady-state motion of the system corresponds to the equilibrium solution when $a' = b' = \phi_1' = \phi_2' = 0$ in the Equations (19)-(22). In order to determine the stability of its equilibrium solution, the Equations (19)-(22) are transformed into the rectangular coordinate system:

$$p_1' = -\frac{1}{2}\xi_1 p_1 - \delta_2 q_1 - \frac{1}{2\omega_1}\mu\omega_2^2(\gamma-1)q_1 - \frac{1}{2\omega_1}\mu\omega_2^2 q_2, \tag{23}$$

$$q_1' = -\frac{1}{2}\xi_1 q_1 + \delta_2 p_1 + \frac{1}{2\omega_1}\mu\omega_2^2(\gamma-1)p_1 + \frac{1}{2\omega_1}\mu\omega_2^2 p_2 + \frac{1}{2\omega_1}F, \tag{24}$$

$$\begin{aligned} p_2' = {} & -(\delta_2 - \delta_1)q_2 + \frac{1}{2\omega_2}\xi\omega_1(1-\gamma)p_1 + \frac{\omega_2}{2} g\left[\sin(\omega_2\tau)p_2 + \cos(\omega_2\tau)q_2\right] - \frac{1}{2(\omega_1^2 - \omega_2^2)}\mu\omega_2^3 q_2 + \frac{\omega_1^2}{2\omega_2} g\gamma\left[\sin(\omega_1\tau)p_1 + \cos(\omega_1\tau)q_1\right] \\ & - \frac{1}{\omega_2}\alpha\left(\frac{3}{8} - \frac{3}{4}\gamma + \frac{3}{8}\gamma^2\right)\left(p_1^2 q_2 - q_1^2 q_2 - 2p_1 p_2 q_1\right) \\ & + \frac{1}{\omega_2}\alpha\left(-\frac{3}{8} + \frac{3}{8}\gamma\right)\left(2p_1 p_2 q_2 - p_2^2 q_1 + q_1 q_2^2\right) \\ & + \frac{1}{\omega_2}\alpha q_2\left[\left(\frac{3}{4} - \frac{3}{2}\gamma + \frac{3}{4}\gamma^2\right)\left(p_1^2 + q_1^2\right) + \frac{3}{8}\left(p_2^2 + q_2^2\right)\right] \\ & + \frac{1}{\omega_2}\alpha q_1\left[\left(-\frac{3}{8} + \frac{9}{8}\gamma - \frac{9}{8}\gamma^2 + \frac{3}{8}\gamma^3\right)\left(p_1^2 + q_1^2\right)\right. \\ & \left. + \left(-\frac{3}{4} + \frac{3}{4}\gamma\right)\left(p_2^2 + q_2^2\right)\right] + \frac{1}{2\omega_2}\omega_1^2\zeta\left[q_2 + \gamma q_1\right], \end{aligned} \tag{25}$$

$$
\begin{aligned}
q_2' = {} & (\delta_2 - \delta_1) p_2 + \frac{1}{2\omega_2} \xi\omega_1 (1-\gamma) q_1 + \frac{\omega_2}{2} g \left[\sin(\omega_2 \tau) q_2 \right. \\
& \left. - \cos(\omega_2 \tau) p_2 \right] + \frac{1}{2(\omega_1^2 - \omega_2^2)} \mu\omega_2^3 p_2 + \frac{\omega_1^2}{2\omega_2} g\gamma \left[\sin(\omega_1 \tau) q_1 \right. \\
& \left. - \cos(\omega_1 \tau) p_1 \right] - \frac{1}{\omega_2} \alpha \left(\frac{3}{8} - \frac{3}{4}\gamma + \frac{3}{8}\gamma^2 \right) \left(p_1^2 p_2 - q_1^2 p_2 + 2 p_1 q_2 q_1 \right) \\
& - \frac{1}{\omega_2} \alpha \left(-\frac{3}{8} + \frac{3}{8}\gamma \right) \left(2 p_2 q_1 q_2 - q_2^2 p_1 + p_1 p_2^2 \right) \\
& - \frac{1}{\omega_2} \alpha q_2 \left[\left(\frac{3}{4} - \frac{3}{2}\gamma + \frac{3}{4}\gamma^2 \right) \left(p_1^2 + q_1^2 \right) + \frac{3}{8} \left(p_2^2 + q_2^2 \right) \right] \\
& - \frac{1}{\omega_2} \alpha q_1 \left[\left(-\frac{3}{8} + \frac{9}{8}\gamma - \frac{9}{8}\gamma^2 + \frac{3}{8}\gamma^3 \right) \left(p_1^2 + q_1^2 \right) \right. \\
& \left. + \left(-\frac{3}{4} + \frac{3}{4}\gamma \right) \left(p_2^2 + q_2^2 \right) \right] - \frac{1}{2\omega_2} \omega_1^2 \zeta \left[p_2 + \gamma p_1 \right],
\end{aligned} \tag{26}
$$

where $p_1 = a\cos\phi_1$, $q_1 = a\sin\phi_1$, $p_2 = b\cos(\phi_1 + \phi_2)$, $q_2 = b\sin(\phi_1 + \phi_2)$.

In order to analyze the stability of the equilibrium solution, perturbation analysis is first performed on the Equations (23)-(26), and the perturbation equation is as follows:

$$
\{\Delta p_1', \Delta q_1', \Delta p_2', \Delta q_2'\}^{\mathrm{T}} = [J] \{\Delta p_1, \Delta q_1, \Delta p_2, \Delta q_2\}^{\mathrm{T}}, \tag{27}
$$

where T stands for transpose matrix, Jacobian matrix. Then, the characteristic equation corresponding to the equilibrium point is expressed as:

$$
\lambda^4 + \delta_1 \lambda^3 + \delta_2 \lambda^2 + \delta_3 \lambda + \delta_4 = 0 \tag{28}
$$

where λ represents the eigenvalue of matrix λ, $\delta_1, \delta_2, \delta_3$ and δ_4 represent the coefficients of the eigenequation. Finally, Rose-Horwitz criterion is used to judge the stability of the equation. Obtain sufficient and necessary conditions for system stability:

$$
\delta_1 > 0, \delta_1\delta_2 - \delta_3 > 0, \delta_3 (\delta_1\delta_2 - \delta_3) - \delta_1^2 \delta_4 > 0, \delta_4 > 0, \tag{29}
$$

The necessary and sufficient conditions for static bifurcation are:

$$
\delta_4 = 0 \tag{30}
$$

The necessary and sufficient conditions for Hopf bifurcation are:

$$
\delta_1\delta_3 > 0, \ \delta_3 (\delta_1\delta_2 - \delta_3) - \delta_1^2 \delta_4 = 0. \tag{31}
$$

The sufficient and necessary condition for the equilibrium solution of Equations (2) and (3) is that the real parts of all eigen roots of the Eigenequation (28) are less than zero; The equilibrium solution of Equations (2) and (3) is unstable if the real part of one of the eigen roots is positive. Moreover, if the real part of the characteristic root changes sign, the system may have a saddle bifurcation, which will lead to a jump phenomenon. Moreover, if the real part of a pair of complex eigen roots changes sign, the system may have a Hope bifurcation, resulting in complex motions such as almost periodic motions.

Dimensionless parameter selection is as follows:

$$\omega_1 = 1.0,\ \omega_2 = 0.8,\ \varepsilon\sigma_1 = -0.2,\ \varepsilon\mu = 0.15,\ \varepsilon\xi_1 = 0.3,\ \varepsilon\xi_2 = 0.3,\ \varepsilon F = 0.1.$$

5. Effect of Cubic Nonlinear Coefficient on Vibration Reduction of System

According to the above analysis, when the feedback gain coefficient $\varepsilon g = 0$, the delay feedback term disappears. In this chapter, the nonlinear dynamic vibration absorber with negative stiffness coefficient h of $\varepsilon\zeta = -0.1$ is taken as an example to analyze the vibration reduction effect of the third nonlinear coefficient b on the dynamic vibration absorber. Figure 2 shows the steady-state amplitude-frequency response curve of the main system with a negative stiffness coefficient $\varepsilon\zeta = -0.1$. H1, H2 represent the Hopf bifurcation point, SN1, SN2, SN3, SN4 represent the Saddle node bifurcation point. The solid line of the black dot represents the stable solution, the solid line of the red dot represents the unstable focus, and the solid line of the blue dot represents other unstable solutions except the unstable focus.

The dimensionless parameters in this chapter are selected as:

$$\omega_1 = 1.0,\ \omega_2 = 0.8,\ \varepsilon\sigma_1 = -0.2,\ \varepsilon\mu = 0.15,\ \varepsilon\xi_1 = 0.3,\ \varepsilon\xi_2 = 0.3,\ \varepsilon F = 0.1.$$

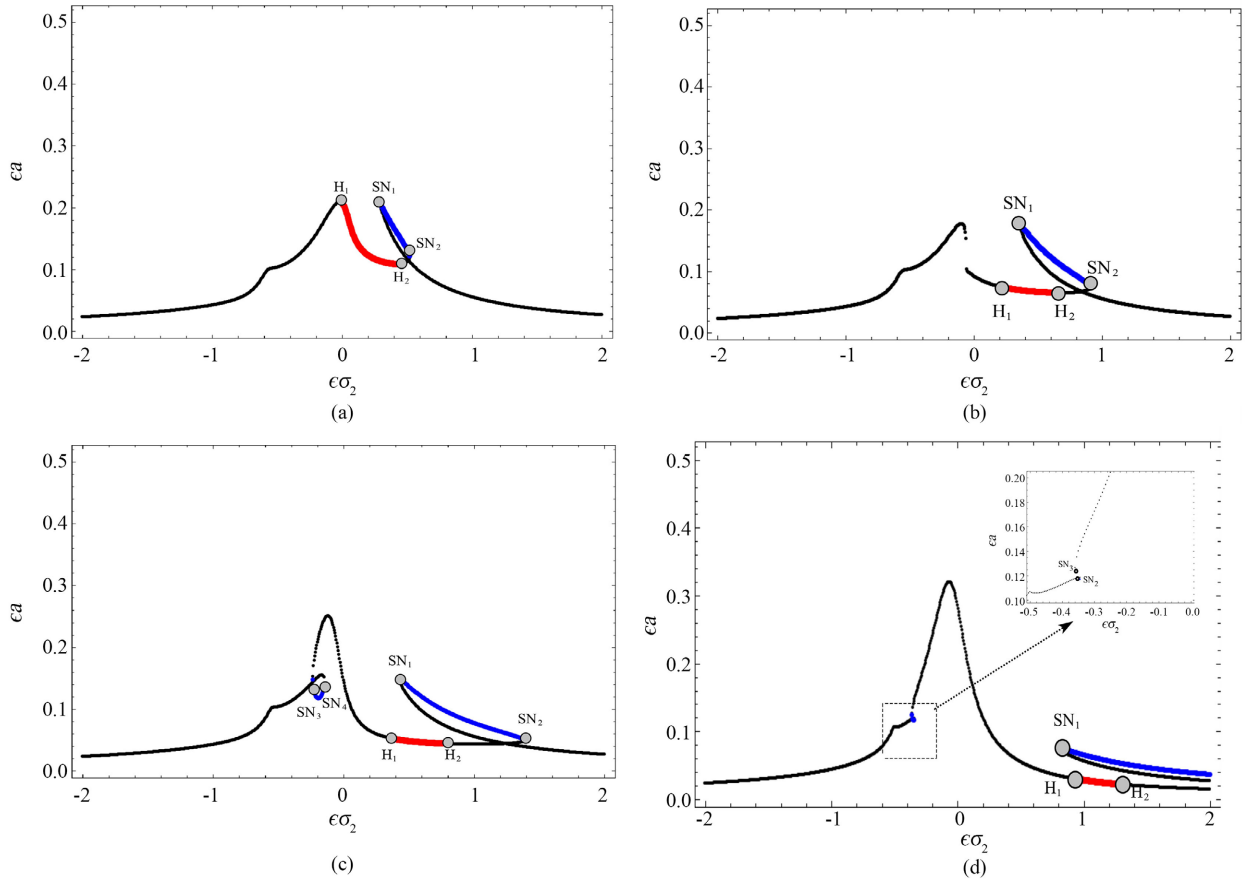

Figure 2. The steady-state amplitude frequency response curve of the main system. (a) $\varepsilon\alpha = 1.7$ (b) $\varepsilon\alpha = 2.5$ (c) $\varepsilon\alpha = 3.6$ (d) $\varepsilon\alpha = 5.5$.

Separate analysis of different values of $\varepsilon\alpha$: As can be seen from **Figure 2(a)**, when the cubic nonlinear coefficient $\varepsilon\alpha = 1.7$, Hope bifurcation occurs in the region from 0.04 to 0.3 of the external tuning parameter $\varepsilon\delta_2$, and saddle junction bifurcation occurs in the region from 0.18 to 0.8 of the external tuning parameter $\varepsilon\delta_2$ to the right of the resonance point, resulting in an unstable region. Because of the existence of Hope bifurcation, the system may have complex almost periodic motion. The saddle-junction bifurcation makes multiple periodic solutions coexist, and the system will jump. As can be seen from **Figure 2(b)**, when the cubic nonlinear coefficient $\varepsilon\alpha$ increases from 1.7 to 2.5, the instability region of the amplitude-frequency response curve due to Hope bifurcation and saddle junction bifurcation increases continuously. By increasing the cubic nonlinear coefficient h to 3.6, it can be seen in **Figure 2(c)** that the branches of unstable solutions intersect with the branches of stable solutions between the two saddle junction bifurcation points SN3 and SN4. When the cubic nonlinear coefficient $\varepsilon\alpha$ is increased to 5.5, the stable region of the amplitude-frequency response curve is increasing.

Through comparative analysis of the four diagrams in **Figure 2(a)**, it is found that although the internal resonance ratio is not strictly equal to 1 due to the internal tuning parameter $\varepsilon\delta_1 \neq 0$, it can be observed that the negative stiffness nonlinear dynamic vibration absorber can effectively control the amplitude of the system at the resonance point. With the increase of the cubic nonlinear coefficient, the amplitude of the main system at the resonance point will decrease to a certain extent, which can be controlled to about 0.1, and the nonlinear vibration reduction effect is very significant. However, it should be noted that the nonlinear dynamic vibration absorber with larger $\varepsilon\alpha$ has a wider vibration attenuation frequency band of its control system than the nonlinear dynamic vibration absorber with smaller $\varepsilon\alpha$, so the selection of $\varepsilon\alpha$ should simultaneously satisfy the requirement that the width of the vibration attenuation band is wide enough and the resonance point replication is small enough.

6. Effect of Time Delay on Vibration Reduction of System

From the above analysis of the nonlinear dynamic vibration absorber, it can be seen that the negative stiffness nonlinear dynamic vibration absorber proposed in this chapter plays a good damping effect near the resonance point. In this chapter, the negative stiffness nonlinear dynamic vibration absorber with cubic nonlinear parameter $\varepsilon\alpha = 0.1$ and negative stiffness coefficient $\varepsilon\zeta = -0.6$ is taken as an example. That is, **Figure 3** analyzes the effect of time-delay feedback control of external tuning parameter $\varepsilon\delta_2 = -0.05$ on vibration reduction of the dynamic system. **Figure 3** shows the amplitude-time delay response curve of the main system under different feedback gain coefficients εg with time-delay coupling negative stiffness dynamic vibration absorber under given parameters. **Figure 3(a)** shows the amplitude-delay response curve of the main system with feedback gain coefficient $\varepsilon g = -0.4$. As can be seen from the figure, the amplitude-delay response curve of the main system will produce two formants and

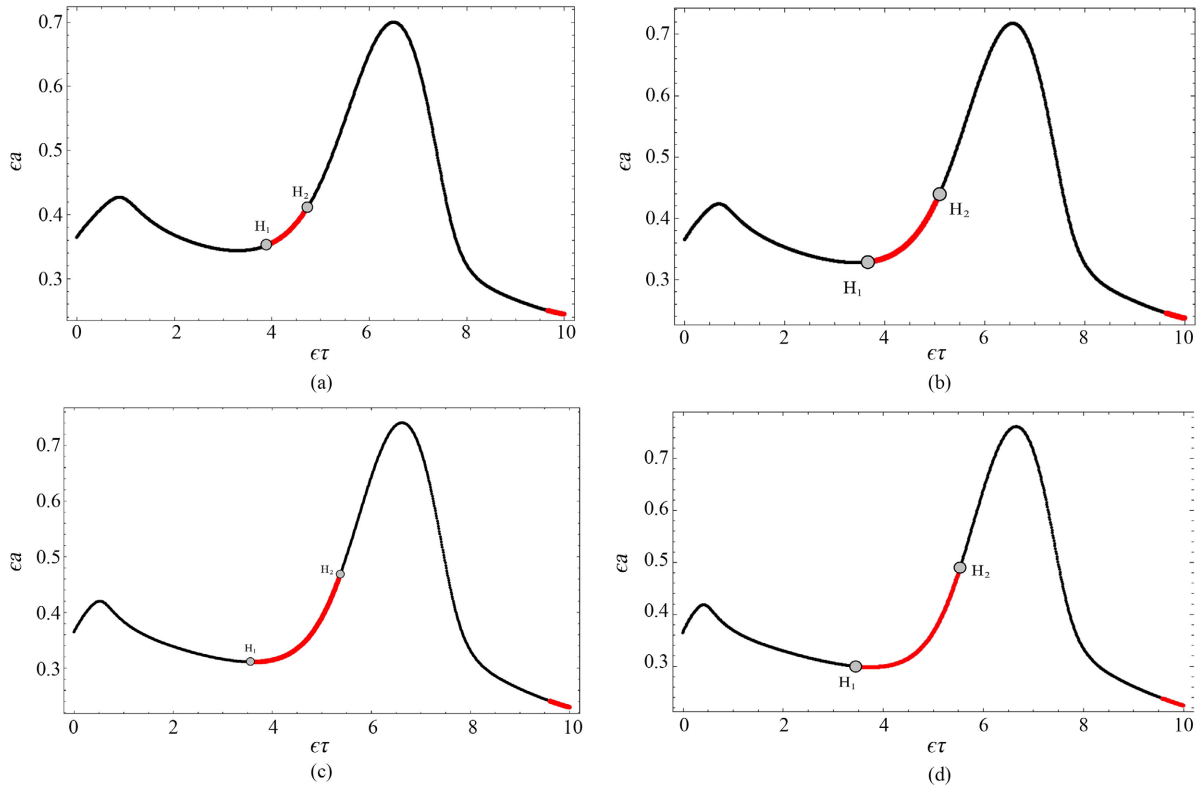

Figure 3. The amplitude time delay response curve of the main system. (a) $\varepsilon g = -0.4$; (b) $\varepsilon g = -0.5$; (c) $\varepsilon g = -0.65$; (d) $\varepsilon g = -0.8$.

one anti-formant in the interval of delay value 0 to 10. Moreover, with the increase of the delay, two Hope bifurcation points H1 and H2 are generated in the amplitude response curve with the delay of about 4.0 to 6.0, and the distance between H1 and H2 also increases with the increase of the absolute value of the feedback gain coefficient. When the time lag is taken between the Hoppe bifurcation points, the system may produce complex almost periodic motion and become unstable, and the dynamic absorber loses the damping effect. As can be seen from the four figures in **Figure 3**, the amplitude of the anti-formant decreases with the increase of the absolute value of the feedback gain coefficient.

7. Influence of Negative Stiffness Coefficient ζ on Vibration Reduction of System

As shown in **Figure 4**. From the analysis of the above two chapters, it can be seen that the time-delay coupled negative stiffness nonlinear dynamic absorber proposed in this chapter plays a good damping effect near the resonance point. In this chapter, a time-delay coupled negative stiffness nonlinear dynamic vibration absorber with cubic nonlinear parameters $\varepsilon\alpha = 1.7$ and delay feedback gain coefficient $\varepsilon g = -0.7$ is taken as an example. As shown in **Figure 4**, the effect of time-delay feedback control at external tuning parameter $\varepsilon\delta_2 = -0.02$ on vibration reduction of dynamic system is analyzed. **Figure 4** shows the amplitude-delay response curves of the main system under different negative stiffness

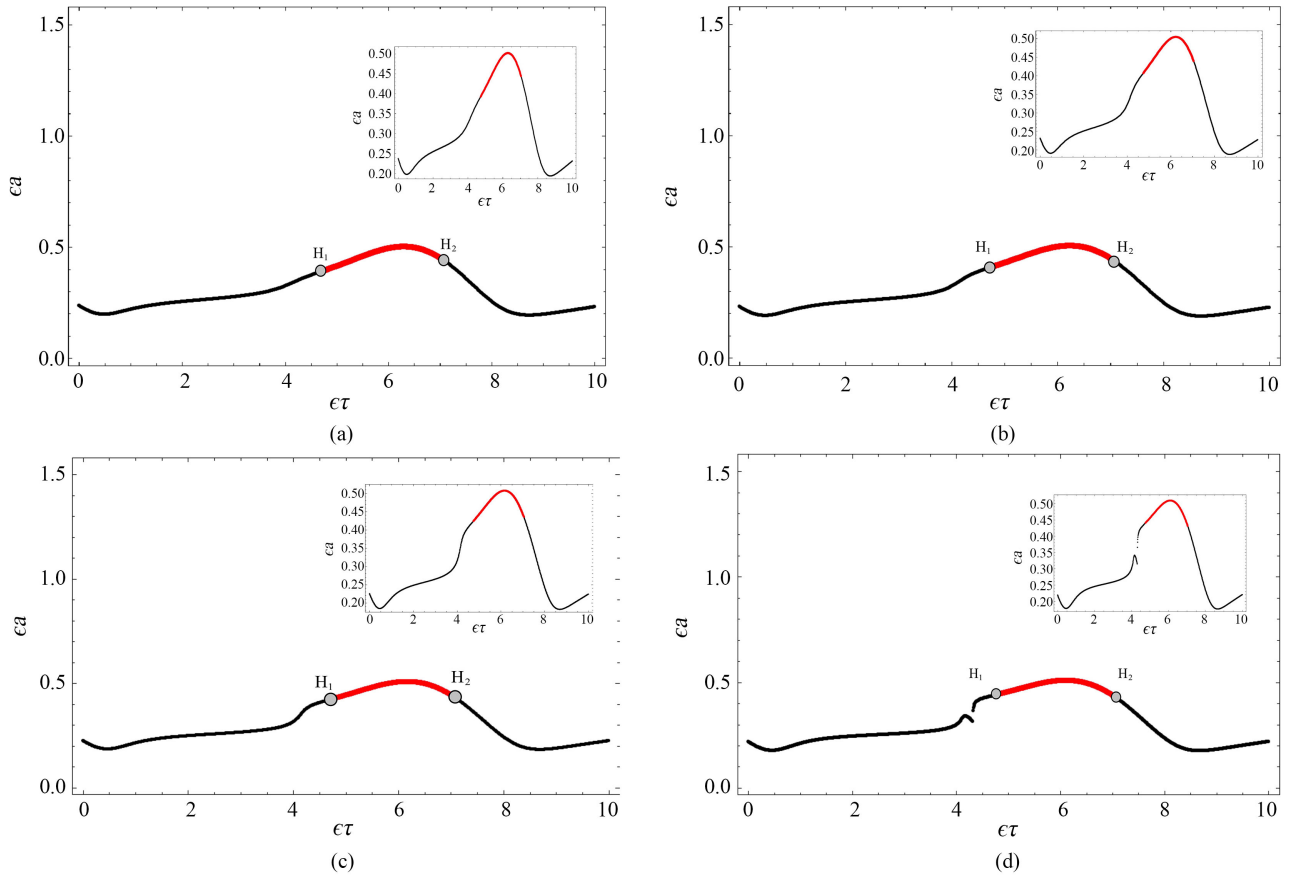

Figure 4. The amplitude time delay response curve of the main system. (a) $\varepsilon\zeta = -0.4$ (b) $\varepsilon\zeta = -0.5$ (c) $\varepsilon\zeta = -0.6$ (d) $\varepsilon\zeta = -0.7$.

coefficients $\varepsilon\zeta$ of the time-delay coupled negative stiffness dynamic vibration absorber with given parameters.

Figure 4(a) shows the amplitude-delay response curve of the main system with a negative stiffness coefficient $\varepsilon\zeta = -0.4$. It can be seen from the figure that the amplitude-delay response curve of the main system will produce one formant and two anti-formants in the interval of time delay ranging from 0 to 10. Moreover, with the increase of time delay, the amplitude-time delay response curve generates two Hope bifurcation points H1 and H2 within the interval of time delay of about 4.0 to 7.0. When the delay takes a value between the Hope bifurcation points, the system will do complex almost periodic motion, resulting in instability of the system and loss of vibration damping effect of the dynamic vibration absorber. It can be seen from the four figures in Figure 4 that under different negative stiffness coefficients, the minimum vibration reduction point exists in the amplitude of the main system under the determined system structure parameters and time-delay feedback control parameters.

8. Conclusions

This chapter mainly studies the influence of time delay and structural parameters on the vibration damping effect of the dynamic vibration absorber with

time-delay coupling and negative stiffness in nonlinear vibration damping system. Taking the dynamic vibration absorber with different structural parameters and control parameters as an example, the influence of the cubic nonlinear coefficient, time-delay control parameter and negative stiffness coefficient on reducing the amplitude of the main system is discussed respectively, and the following conclusions are obtained:

1) The vibration reduction effect of the nonlinear dynamic vibration absorber is very good at the resonance point of the main system and an area near it, and when $\varepsilon\alpha$ is increased to a certain level, the stability area of the system is constantly increasing.

2) The amplitude curve of the main system of the nonlinear dynamic vibration absorber will produce Hope bifurcation and saddle bifurcation in the region far from the resonance point, so that the system will produce almost periodic motion and jumping phenomenon.

3) For the nonlinear dynamic vibration absorber whose structural parameters are determined, delay feedback control can be adopted to control the amplitude of the main system.

4) For different negative stiffness coefficients, under the determined system structure parameters and time-delay feedback control parameters, there is a minimum vibration reduction point in the amplitude of the main system.

Conflicts of Interest

The authors declare no conflicts of interest regarding the publication of this paper.

References

[1] Hermann, F. (1909) Device for Damping Vibrations of Bodies.

[2] Payne, M.L., Abbassian, F., Eng, C., *et al.* (1995) Drilling Dynamic Problems and Solutions for Extended-Reach Operations.

[3] Asami, T. and Nishihara, O. (2002) H_2 Optimization of the Three-Element Type Dynamic Vibration Absorbers. *Smart Structures and Materials* 2002: *Damping and Isolation*, Himeji.

[4] Asami, T. and Nishihara, O. (2002) Closed-Form Solutions to the Exact Optimizations of Dynamic Vibration Absorbers (Minimizations of the Maximum Amplitude Magnification Factors). *Journal of Vibration and Acoustics*, **124**, 576-582.

[5] Peng, X.H. and Chen, S.N. (1995) Research on Stability and Application of Parallel Structures with Positive and Negative Stiffness. *Vibration*: *Test and Diagnosis*, **15**, 14-18.

[6] Peng, H.B., Shen, Y.J. and Yang, S.P. (2015) Parameter Optimization of a New Dynamic Vibration Absorber with Negative Stiffness Elements. *Chinese Journal of Mechanical Mechanics*, **47**, 320-327.

[7] Wang, X.R., Shen, Y.J., Yang, S.P., *et al.* (2017) Parameter Optimization of Three-Element Dynamic Vibration Absorber with Negative Stiffness Element. *Journal of Vibration Engineering*, **30**, 8.

[8] Hao, Y., Shen, Y.J., Yang, S.P., *et al.* (2019) Parameter Optimization of Maxwell

Model Dynamic Vibration Absorber with Negative Stiffness Device. *Journal of Vibration and Shock*, **38**, 6.

[9] Xing, Z.Y. (2020) Realization of Negative Stiffness and Optimal Design of New Dynamic Vibration Absorber. Shijiazhuang Railway University, Shijiazhuang.

[10] Chen, J., Sun, W.G., Wu, Y.J., *et al.* (2020) Beam Response Minimization Based on Inertial Negative Stiffness Dynamic Vibration Absorber. *Journal of Vibration and Shock*, **39**, 8.

[11] Li, Y.S. (2021) Research on Performance of Magnetic Liquid Second-Order Buoyancy Damper. North China University of Water Resources and Electric Power, Zhengzhou.

[12] Li, Y. (2022) Design and Research of Rail Dynamic Vibration Absorber Based on Particle Damping Mechanism. *Railway Construction Technology*, No. 4, 41-45.

[13] Yang, G., Wang, S., Zheng, C.J. and Bi, C.X. (2022) Dynamic Vibration Absorber with Multiple Dry Friction Damping of Rotor and Its Vibration Damping Characteristics. *Journal of Aerodynamics*.

[14] Xiong, B., Chen, W.X., Liu, G., Yu, Y. and Cheng, Q.-Y. (2022) Research and Test on Vibration Absorption Performance of Two-Wire Pendulum Dynamic Vibration Absorber at Propeller Hub. *Science and Technology Innovation*, No. 5, 43-45.

[15] Olgac, N. and Holm-Hansen, B.T. (1994) A Novel Active Vibration Absorption Technique: Delayed Resonator. *Journal of Sound and Vibration*, **176**, 93-104. https://doi.org/10.1006/jsvi.1994.1360

[16] Zhao, Y.Y. and Xu, J. (2012) Using the Delayed Feedback Control and Saturation Control to Suppress the Vibration of the Dynamical System. *Nonlinear Dynamics*, **67**, 735-753. https://doi.org/10.1007/s11071-011-0023-5

[17] Sun, Y.X. and Xu, J. (2015) Experiments and Analysis for a Controlled Mechanical Absorber Considering Delay Effect. *Journal of Sound and Vibration*, **339**, 25-37. https://doi.org/10.1016/j.jsv.2014.11.005

[18] Chen, L.X. and Cai, G.P. (2008) Experimental Research on Active Control of Rotating Flexible Beam with Time Delay. *Chinese Journal of Mechanical Mechanics*, No. 4, 520-527.

[19] Chen, L.X. and Cai, G.P. (2009) Experimental Study on Time-Delay Variable Structure Control of Forced Vibration of Flexible Beams. *Chinese Journal of Mechanical Mechanics*, **41**, 410-417.

[20] Fu, W.Q., Pang, H. and Liu, K. (2017) Modeling and Stability Analysis of Semi-Active Suspension with Delayed Ceiling Damping. *Mechanical Science and Technology for Aerospace Engineering*, **36**, 213-218.

[21] Zhu, K., Ren, C.B., Wang, F. and Qu, Y.W. (2016) Research on Vibration Reduction of 1/4 Vehicle Model with Time-Delay Feedback Control. *Journal of Shandong University of Technology* (*Natural Science Edition*), **30**, 31-35.

[22] Yan, G., Fang, M.X., Dong, T.F. and Ji, R.J. (2018) Delay Feedback Control of Vehicle Suspension System Based on State Transformation Method. *Transactions of the Chinese Society of Agricultural Engineering*, **34**, 54-61.

[23] Zhao, Y.Y. and Huang, X.W. (2020) Vibration and Active Control of Semi-Active Suspension System for High-Speed Train. *Science Technology and Engineering*, **20**, 11794-11802.

[24] Wu, K.W., Ren, C.B., Lu, H., Cao, J.S. and Sun, Z.C. (2022) Research on Passenger Vibration Attenuation of 1/4 Vehicle Model Based on Time-Delay Feedback Control. *Science Technology and Engineering*, **20**, 12158-12165. (In Chinese)